



Lasers in Manufacturing Conference 2015

Experimental and Analytical Description of the Multi Wavelength Remote Laser Ablation Process at Fiber Reinforced Polymers

A.Fürst^{a,b}, D. Hipp^b, M. Rose^{a,b}, A. Klotzbach^a, J. Hauptmann^a, A. Wetzig^a,
E. Beyer^{a,b}

^aFraunhofer IWS Dresden, Winterbergstraße 28, 01277, Dresden, Germany

^bTechnische Universität Dresden, 01062, Dresden Germany

Abstract

To increase the acceptance of fibre reinforced polymers (FRP) in the industry, near net shape preforms with a minimum of material consumption are required. This should be accompanied by appropriate, fast and flexible processes. The remote laser processing expands the area of possible kinds of processing strategies, wherefore the laser can be a tool for the future. But the development of remote laser processing is accompanied with the understanding of the interaction between tool and material. Laser cutting processing of FRP is an ambitious process because of the inhomogeneity of both the reinforcement material and the polymer matrix material. The present paper shows an experimental set up for combining beam radiation with wavelengths of 1.07 μm and 10.6 μm . First results on carbon fiber reinforced polymers prove the increasing efficiency.

Macro Processing; Remote Laser Beam Processing; System Technology; CFRP; FRP

1. Introduction

One of the main challenges in the field of composite materials is the improvement and optimization of existing production processes and procedures. For instance, near-net-shape preforms are used to minimize the material consumption. In addition thermoplastic matrices are used to decrease the cycle time of the production processes (LÄSSIG, 2012). Several investigations have shown that the application of laser processing as a wear and force free tool is appropriate to face the limitations, given by conventional processes like mechanical milling or water jet cutting (FUCHS u. a., 2013; STOCK u. a., 2012). The development of remote laser processing is strongly connected with the knowledge of the material properties under consideration of laser

beam radiation. Especially carbon fiber reinforced materials (CFRP) are characterized by inhomogeneity in heat conductivity and sublimation temperature for matrix and fiber material. Because of high fiber sublimation temperatures (carbon fiber $\approx 3700^{\circ}\text{C}$) and high heat conductivity along the fibers (up to $49 \text{ W/m}\cdot\text{K}$) on one hand and low decomposition temperatures of the matrix material and the coating of the fibers ($300 - 700^{\circ}\text{C}$) on the other. Furthermore, the significantly different absorption behavior of the fiber and the matrix material is an aggravating factor. Prior investigations have shown a drastically difference of absorption behavior between the reinforcement material and the polymer matrix (FÜRST u. a., 2013). The analysis figured out a significant raise of absorbed proportion of the irradiated laser beam at a wavelength of $\lambda = 1.09 \mu\text{m}$ at high fiber volume content. Adding carbon black to the matrix is one possible approach to unify the absorption behavior of both materials, when processing with an emission wavelength in the range of $1.06 - 1.07 \mu\text{m}$ (STOCK u. a., 2012). High intensities are needed to evaporate the reinforcement material of FRP, wherefore brilliant beam sources with a wavelength of $\lambda = 1.09 \mu\text{m}$ are suitable for (KLOTZBACH u. a., 2013; SCHNEIDER u. a., 2013; STOCK u. a., 2014). Here the focusability of the beam radiation is a major key for processing. The focusability is characterized by the beam parameter product (BPP), what is calculated as the product of its diameter d_f at the beam waist and his divergence (HÜGEL & GRAF, 2009; LÜTKE, 2011). It is known that the beam of a CO_2 laser with his emission wavelength of $\lambda = 10,6 \mu\text{m}$ can achieve a minimum $\text{BPP} = 3,4 \text{ mm mrad}$. The achievable BPP within the range of wavelength about $\lambda = 1.07 - 1.09 \mu\text{m}$ can be 0.35 mm mrad . That leads, depending on the field of application to very small focal diameter. To consider the absorption behavior as well as the significant differences of the thermal properties of both materials the combination of two laser beams with wavelengths of $1.09 \mu\text{m}$ and $10.6 \mu\text{m}$ is a promising approach. Therefore, a beam combination device was developed and implemented into laboratory scale.

2. Laboratory set up for beam combination

Figure 1 shows the laboratory setup for wavelength combination of a CO_2 – slab laser (3 kW cw) and a solid-state-laser (1 kW cw). Within this scheme the solid state laser beam path (red) and the CO_2 – laser path (yellow) have to be combined and imaged at the same focusing point. The solid state laser beam is reflected by a dichroic mirror under an angle of 14° . This mirror transmits the CO_2 beam. An adaptive mirror for the CO_2 beam realizes the focal position adjustment. This enables the adjustment of the spot ratio between CO_2 and solid state laser.

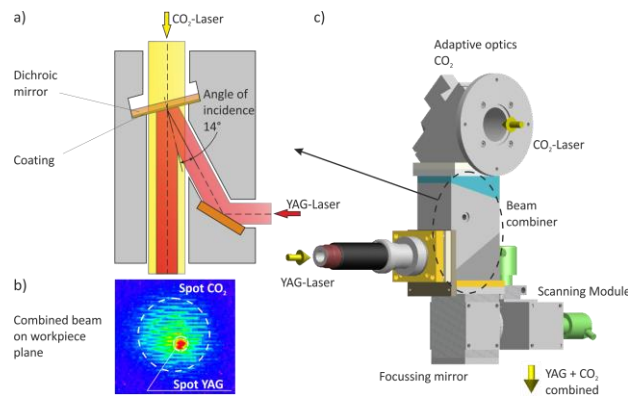


Figure 1 (a) Cross section of laboratory set up, (b) Cross section of measured intensity distribution, (c) Multiwavelength equipment

The wavelength combined and focused beam is then deflected by a fast mirror system based on galvanometer scanners. Both beam sources are operated in cw- mode. Further investigations have shown a

more efficient ablation behavior compared to pulsed beam sources (KLOTZBACH u. a., 2013). Fundamental beam parameters are given in Table 1.

Table 1 Fundamental beam parameters

Parameter	CO ₂ - Laser	Solid state Laser
Wavelength λ [μm]	10.6	1.09
Power P_L [kW]	1- 3	1-1.8
Raw beam diameter D_{raw} [mm]	14	
Fiber diameter D_k [μm]		20
Collimation focal length f_k [mm]		160
Focal length of focussing mirror f_f [mm]	400	400

The resulting spot radius for the CO₂ beam is calculated by:

$$d_{f,\text{CO}} = \frac{M^2 \times 4 \times \lambda \times f_f}{\rho \times D_{\text{raw}}} \quad (1)$$

and for the solid state beam:

$$d_{f,\text{SSL}} = \frac{D_k \cdot f_f}{f_k} \quad (2)$$

The beam propagation of each focused beam is measured by a Focus Monitor (Primes GmbH), below beam exit of the scanning module. Comparing the calculated beam and the measured beam both values are in good accordance despite the complex beam guidance. The difference between the z- position of the beam is compensated by the adaptive mirror.

Table 2 Result of beam propagation measurement

Parameter	CO ₂ - Laser	Solid state- Laser
Wavelength λ [μm]	10.6	1.09
86% radius of beam waist r_0 [μm]	256	27
Z- Position of focus [mm] (below scanning module)	233	220
Beam parameter product [mm mrad]	3.4	0.6
Rayleighlength z_r [mm]	20.5	1.7

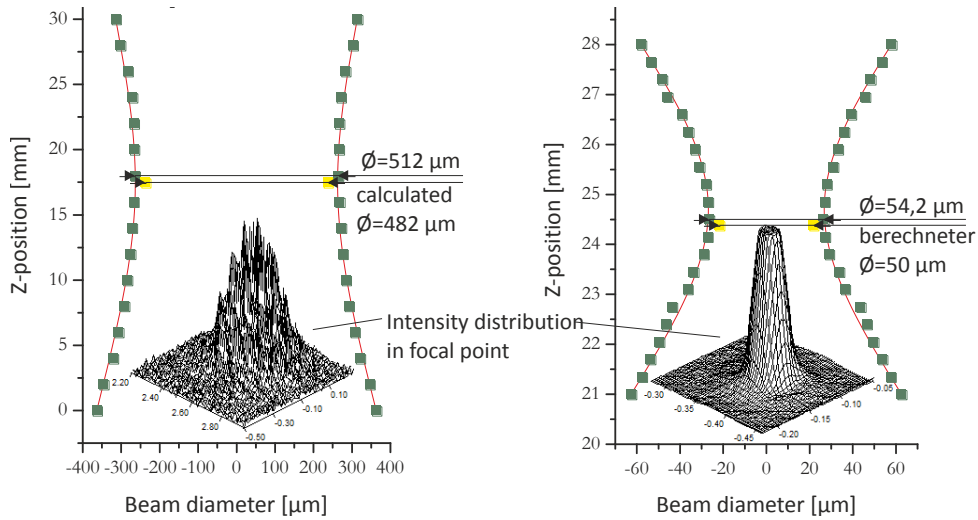


Figure 2 Calculated and measured beam propagation, (a) CO₂ beam, (b) solid state laser beam

3. Experimental determination of cutting efficiency

3.1. Material and description of experiments

First results were represented on carbon reinforced polymer (CFRP) with a thickness of 5 mm and a fiber volume content of $\varphi \approx 60\%$. The cuts were arranged perpendicular to the fiber direction. This set up constitutes one of the most ambitious cutting tasks. To perform a cut the carbon fiber has to be evaporated completely. Furthermore, required energy for evaporation is removed from the cutting zone, due to the thermal heat conductivity of the carbon fiber (LIEBELT, 1998).

Table 3 Characteristic thermal properties of the CFRP (FLEMMING u. a., 1995; HESSE, 1995; SCHÜRMANN, 2005)

Material	Heat Capacity [J/(kg*K)]	Glass transition Temperature [°C]	Evaporation Temperature [°C]	Thermal heat Conductivity [W/(m*K)]
Epoxy resin	1400	140	400- 600	0.21
Carbon fiber (high tenacity)	710		3600	78.4*

* longitudinal to fiber direction

To investigate process efficiency the ablation behavior has to be determined. Therefore a complete thru cut was not necessary. The influence of ablation depths on the cutting efficiency is taken into consideration due to number of repetitions at a constant beam power P_L and spot velocity v_v . The focal position is set to 1/3 of material thickness outbound of the top of material. The delay, determined by (STOCK u. a., 2012) could be confirmed by pretests. Hence for all trials a constant delay of 1000 ms between each repetition is provided. The parameters for single laser cutting are shown in Table 4.

Table 4 Experimental parameters for single laser cutting

Parameter	CO ₂ - Laser/ Solid state- Laser
Power P _L [kW]	1.2
Spot velocity v _v [m/s]	1
Number of repetitions	5, 10, 20

Furthermore the influence of absorption behavior as a function of wavelength has to be determined. Therefore the spot radii of both beams are set constant. By defocusing the solid state beam the intensity was adapted to the value of the CO₂ beam.

For wavelength synchronous processing the total laser beam power is set constant to 1200 W. The proportion of laser beam power of each beam source is varied from 25%, 50% and 75% of the total laser beam power (Table 5).

Table 5 Experimental parameters for synchronous laser cutting

Parameter	CO ₂ - Laser	Solid state- Laser (SSL)
Wavelength λ [μm]	10.6	1.09
Power P _L [kW] synchronous 25 % CO- 75% SSL	0.3	0.9
Power P _L [kW] synchronous 50 % CO- 50% SSL	0.6	0.6
Power P _L [kW] synchronous 75 % CO- 25% SSL	0.9	0.3
Spot velocity v _v [m/s]		1
Number of repetitions		5, 10, 20

3.2. Analytical description of cutting efficiency

The experimentals are accompanied by an analytical description. Therefore the specific point energy (SPE), which is already introduced by (SUDER, 2012) is suitable to describe the process:

$$E_{SP} = \iint I(x, y) \times t_{i,P} dx dy \quad (3)$$

Equation (6) describes the Energy, which is delivered by the beam within a given interaction time between beam and material:

$$t_{i,P} = \frac{d_f}{v_v} \quad (4)$$

For a beam with a Gaussian intensity distribution I₀ at a spot area A_{SP} and a constant t_{i,P}, the SPE is given by (SUDER, 2012):

$$E_{SP} = I_0 \times t_{i,P} \times A_{SP} = \frac{P_L \times d_f}{v} \quad (5)$$

Typically cutting of FRP is an ablation process. A complete thru cut is performed by a cyclic material removal until the cutting kerf is formed completely (KLOTZBACH, 2011; SCHNEIDER u. a., 2013; STOCK u. a., 2012). To consider that, the effective velocity v is quotient of laser spot velocity v_V and number of repetitions n_Z . The SPE is then given by:

$$E_{SP} = \frac{P_L \times d_f \times n_Z}{v_V} \quad (6)$$

Considering the combination of both beams, the SPE has to be adapted in the form of:

$$E_{SP} = \frac{n_Z}{v_V} \cdot (p_{SSL} \cdot P_{tot} \cdot d_{f,SSL} + p_{CO} \cdot P_{tot} \cdot d_{f,CO}) \quad (7)$$

Where p_{SSL} and p_{CO} is the proportion of single laser beam power at the total laser beam power P_{tot} . Besides of the SPE another process-descriptive parameter is the cutting efficiency R_{eff} (LEONE, 2013). R_{eff} is described as the ratio between ablation volume ΔV_{SF} and impacting energy E_{tot}

$$R_{eff} = \frac{\Delta V_{SF}}{E_{tot}} \quad (8)$$

The impacting energy E_{tot} is calculated by the mean power of the beam source P_L and the total interaction time between laser beam and material $t_{i,tot}$.

$$E_{tot} = P_L \cdot t_{i,tot} = P_m \cdot n_Z \cdot \frac{l_{SF}}{v_V} \quad (9)$$

Where l_{SF} describes the length of the cutting path and v_V the spot velocity for each repetition and n_Z the number of repetitions. The ablation volume ΔV_{SF} is determined by the evaluation of cross sections of each cutting kerf. Here the area of complete evaporated material is taken into account .

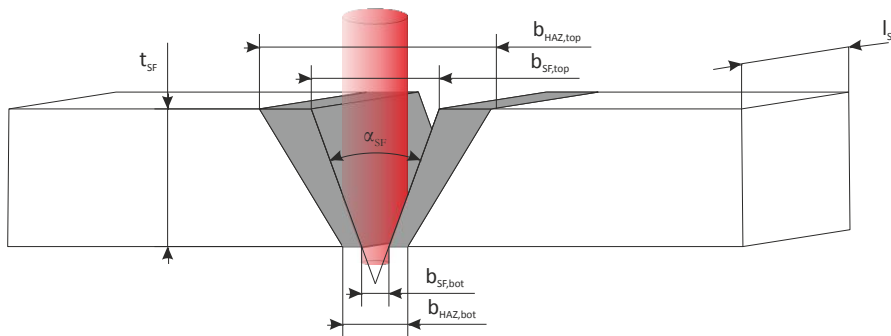


Figure 3 Schematic representation of ablation kerf

4. Results and Discussion

In the following the results for the characteristic single laser ablation behaviour for a constant beam power and spot velocity with varying number of repetitions are shown (Table 4). Figure 4 shows exemplary cross sections of the single laser ablation behaviour. Compared to the laser ablation kerf, generated by the solid state laser, a wider ablation kerf characterized by a huge aperture on the top of the material is generated by the CO₂ beam. Furthermore the CO₂ ablation kerf is characterized by geometrically deterioration of the kerf mainly at the top of the material. Moreover the huge spot diameter of the CO₂ beam leads to a long interaction time between beam and material. Hence much more SPE is needed to achieve ablation volumes, which are comparable to the solid state laser (Figure 5). Resulting in a significantly larger pronounced heat affected zone (HAZ). Due to the small spot diameter of the solid state laser, higher intensities can be achieved. In addition it is assumed, that the smaller beam propagation of the solid state laser leads to a smaller volume of material that has to be ablated. Both ablation kerfs show a deviation of the direction of ablation and the beam orientation, which is perpendicular to the top of material. It is assumed that increasing multiple reflections, caused by a narrowing ablation kerf and the interaction between evaporated material and the beam can be a reason for that.

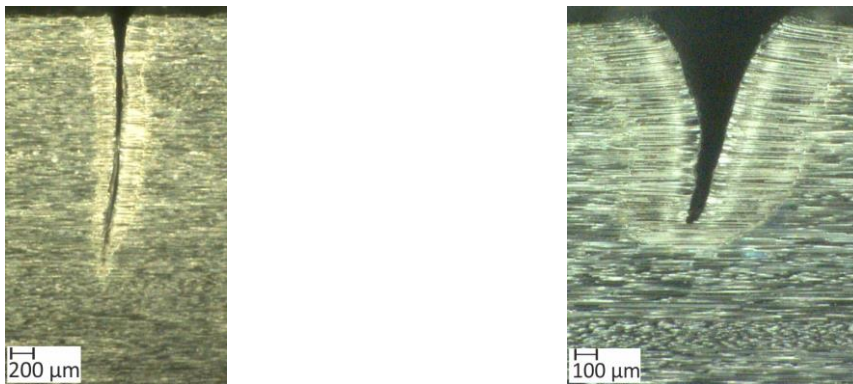


Figure 4 Characteristic ablation kerf, (a) CO₂ laser beam, (b) solid state laser beam ($P_L= 1.2$ kW, $v_v= 1$ m/s, $n= 20$)

Comparable ablation behaviour can be determined, when processing with similar intensities (Figure 5). Obviously the intensity, which can be mapped on the material, has more influence onto ablation behaviour than the proportion of absorbed laser power. When increasing the intensity by reduction of the spot diameter, less SPE is required to achieve comparable ablation volumes. Since the focal diameter affects the interaction time and is directly proportional to the SPE, the decreasing values for SPE are set compulsory. The use of synchronous processing shows a marginally minor SPE, which is necessary to achieve comparable ablation volumes.

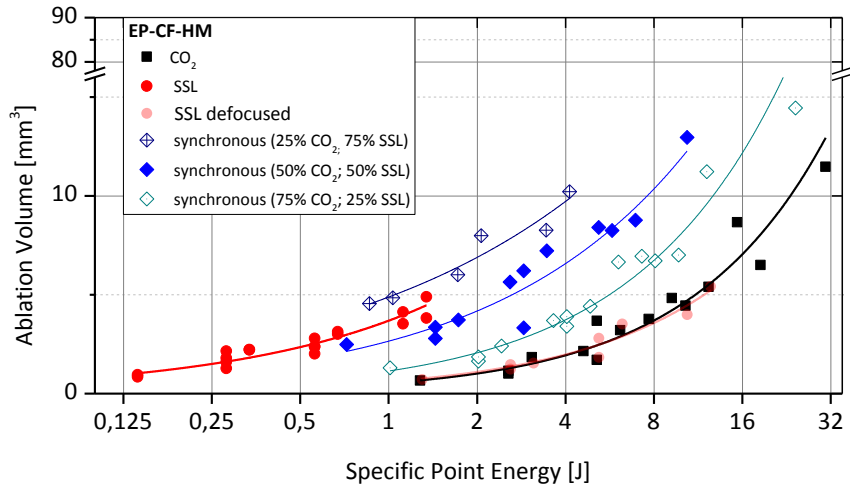


Figure 5 Ablation volume subjected to SPE for high modulus carbon fiber

Here the statements of SPE are not sufficient to constitute the ablation behavior, because a decreasing spot radius leads to an increasing SPE in any case. For this reason the cutting efficiency as a function of ablation depth is presented in Figure 6. Here the number of passes is the dimension of ablation depth. The application of synchronous radiation with a beam power percentage of 25 % of CO₂ and 75 % of solid state laser radiation leads to a significant increasing of ablation efficiency. It is assumed that a considerably proportion of polymer matrix material is evaporated by the radiation with the wavelength of $\lambda = 10.6 \mu\text{m}$. That leads to a significant rise of fiber volume content within the ablation area. Prior investigations have shown that an increasing fiber volume content leads to an increasing proportion of absorbed laser power at a wavelength of $\lambda = 1.09 \mu\text{m}$ (FÜRST u. a., 2013).

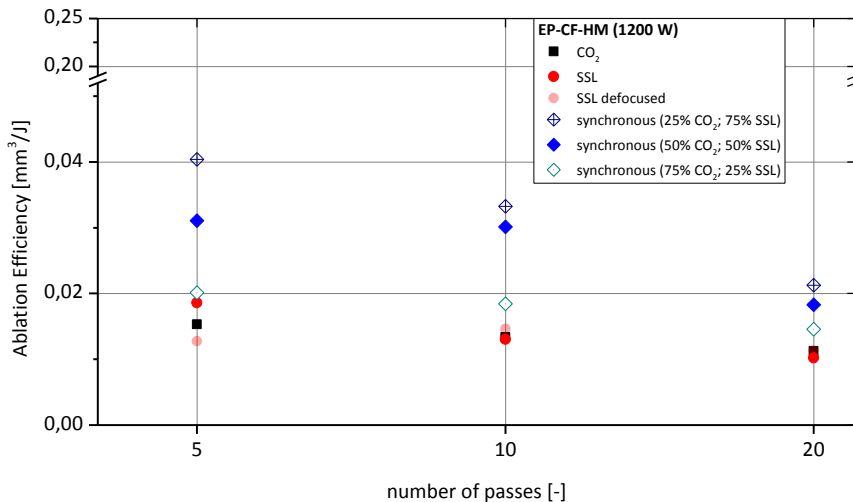


Figure 6 Ablation efficiency subjected to number of passes for high modulus carbon fiber

Comparable to single CO₂- processing a widening of the aperture at the top of the material and a rising geometrically deterioration is recognizable at increasing percentage of CO₂ laser power (Figure 7). This is accompanied with an increasing SPE as a result of proportional enhanced interaction time between combined laser beam and material (Figure 5), which leads to a much more pronounced HAZ.

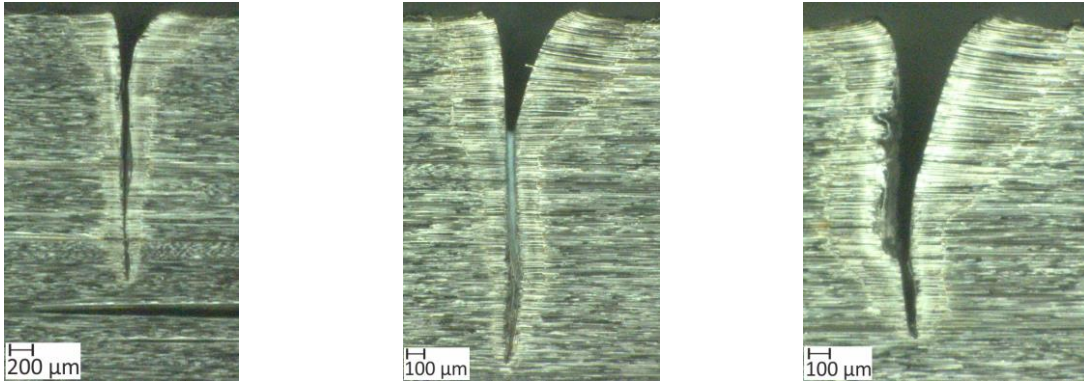


Figure 7 Cross sections of synchronous ablation strategies with increasing percentage of CO₂ laser power, (a) 25 %, (b) 50 %, (c) 75% (CFRP, $P_{\text{tot}}= 1.2 \text{ kW}$, $v_f=1 \text{ m/s}$, $n= 20$)

5. Conclusion

A laboratory set up for combining two beams with radiation of $\lambda= 10.6$ and $\lambda= 1.09 \mu\text{m}$ has been introduced within this paper. The different focal lengths can be adjusted by an adaptive optic within the optical path of the CO₂ beam. Here, the optimum absorption behaviour of the polymeric matrix is utilized when irradiated with radiation of $\lambda= 10.6 \mu\text{m}$ in order to vaporize the polymer matrix. At the same time a sufficiently high intensity can be achieved by the good focusability of the solid-state laser beam ($\lambda= 1.09 \mu\text{m}$) to sublimate the reinforcement fiber content. Fundamental strategies like simultaneous treatment have been carried out to evaluate the process efficiency. First results have shown that a laser beam power combination of 25% CO₂ and 75% solid state laser is suitable to increase the cutting efficiency compared to single- SSL cutting by 50%. It is assumed that vaporization of the polymer matrix leads to an increasing fiber volume content within the HAZ. In addition evaporator residues, consisting a high proportion of carbon deposits at the cutting edge. Both leads to an increasing absorption capacity of radiation at a wavelength of $\lambda= 1.09\mu\text{m}$. Further investigations have to confirm the assumptions established within this paper. The influence of thermal heat conductivity can be minimized by the usage of thermal isotropic, short-fibered material. Furthermore the influence of glass fiber reinforced polymers on the cutting efficiency has to be examined.

6. Acknowledgements

Part of this research was funded by the “Deutsche Forschungsgemeinschaft DFG” within the Collaborative Research Centre SFB 639 of TU Dresden, Textile-reinforced composite components for function-integrating multi-material design in complex lightweight applications, project part: D4.

Literature

FLEMMING, MANFRED ; ROTH, SIEGFRIED ; ZIEGMANN, GERHARD: *Faserverbundbauweisen: Fasern und Matrices, Fasern und Matrices*. Berlin [u.a.] : Springer, 1995 — ISBN 3-540-58645-8

FUCHS, A. N. ; SCHOEBERL, M. ; TREMMER, J. ; ZAEH, MICHAEL F.: Laser Cutting of Carbon Fiber Fabrics. In: *Physics Procedia* Bd. 41 (2013), S. 372–380

FÜRST, A. ; KLOTZBACH, A. ; HÜHNE, S. ; HAUPTMANN, J. ; BEYER, E.: Remote Laser Processing of Composite Materials with Different Opto–Thermic Properties. In: *Physics Procedia* Bd. 41 (2013), S. 389–398

HESSE, DIETMAR: *Abtragen und Schneiden von Kohlefaser-verbundwerkstoffen mit Excimer-Laserstrahlung, Fortschritt-Berichte / VDI Fertigungstechnik*. Bd. Nr. 333. Als Ms. gedr. Aufl. Düsseldorf : VDI-Verl., 1995 — ISBN 3183333023

HÜGEL, HELMUT ; GRAF, THOMAS: *Laser in der Fertigung: Strahlquellen, Systeme, Fertigungsverfahren, Strahlquellen, Systeme, Fertigungsverfahren*. 2. Aufl. Wiesbaden : Vieweg+Teubner, 2009 — ISBN 978-3-8351-0005-3

KLOTZBACH, A.: Laser cutting of carbon fiber reinforced polymers using highly brilliant laser beam sources. In: : Elsevier, 2011 — ISBN 18753884, S. 572–577

KLOTZBACH, A. ; FÜRST, A. ; HAUPTMANN, J. ; BEYER, E.: Investigations on laser Remote cutting of tailored fiber reinforced structures. In: *The second International Symposium on Laser Processing for CFRP and Composite Materials* (2013)

LÄSSIG, R.: Serienproduktion von hochfesten Faserverbundbauteilen, Perspektiven für den deutschen Maschinen- und Anlagenbau, Studie Roland Berger 2012, Roland Berger (2012)

LEONE, C.: Investigation of CFRP laser milling using a 30 W Q-switched Yb:YAG fiber laser: Effect of process parameters on removal mechanisms and HAZ formation. In: *Composites Part A-applied Science And Manufacturing* Bd. 55 (2013), S. 129–142

LIEBELT, STEFAN: *Analyse und Simulation des Laserstrahlschneidens von Faserverbundkunststoffen, Berichte aus dem Produktionstechnischen Zentrum Berlin*. Berlin : PTZ [u.a.], 1998 — ISBN 3-8167-5190-3

LÜTKE, MATTHIAS: *Entwicklung des Remote-Laserstrahlschneidens metallischer Werkstoffe*. Stuttgart : Fraunhofer-Verl., 2011 — ISBN 978-3-8396-0359-8

SCHNEIDER, F. ; WOLF, N. ; PETRING, D. ; EMMELMANN, C.: High power laser cutting of fiber reinforced thermoplastic polymers with cw- and pulsed lasers. In: : Elsevier, 2013, S. 415–420

SCHÜRMMANN, HELMUT: *Konstruieren mit Faser-Kunststoff-Verbunden*. Berlin; Heidelberg : Springer, 2005 — ISBN 3540402837

STOCK, JOHANNES W. ; ZAEH, MICHAEL F. ; SPAETH, JUSTINIAN P.: Remote laser cutting of CFRP: influence of the edge quality on fatigue strength. In: DORSCH, F. (Hrsg.): , 2014, S. 89630T

STOCK, JOHANNES ; ZAEH, MICHAEL F. ; CONRAD, MARKUS: Remote Laser Cutting of CFRP: Improvements in the Cut Surface. In: *Physics Procedia* Bd. 39 (2012), S. 161–170

SUDER, W. J.: Investigation of the effects of basic laser material interaction parameters in laser welding. In: *Journal of Laser Applications* Bd. 24 (2012), Nr. 3, S. 032009